Scripta Materialia 159 (2019) 123–127

Contents lists available at ScienceDirect

Scripta Materialia

journal homepage: www.elsevier.com/locate/scriptamat

Radiation-resistant nanotwinned austenitic stainless steel

G. Meric de Bellefon [a,*], I.M. Robertson [b], T.R. Allen [a], J.-C. van Duysen [c,d], K. Sridharan [a,b]

[a] Department of Engineering Physics, University of Wisconsin, Madison, USA
[b] Department of Materials Sciences, University of Wisconsin, Madison, USA
[c] Department of Nuclear Engineering, University of Tennessee, Knoxville, USA
[d] EDF—Centre de Recherche des Renardieres, Moret sur Loing, France

ARTICLE INFO

Article history:
Received 21 August 2018
Received in revised form 13 September 2018
Accepted 16 September 2018
Available online xxxx

Keywords:
Austenitic stainless steel
Nanotwinned
Irradiation
Deformation twinning
Void swelling

ABSTRACT

A key strategy to increase the radiation resistance of materials has been to introduce a high density of interfaces that can act as sinks for radiation-induced defects. Twin boundaries are a type of interface that can be introduced through deformation but are usually considered to be ineffective sinks. Using heavy ion irradiation and transmission electron microscopy, this study investigates the influence of a high area per unit volume of twin boundaries on the radiation-induced swelling response of an austenitic stainless steel. The study shows that swelling can be suppressed in regions containing a high density of closely-spaced deformation twin boundaries.

Under neutron irradiation, metals and alloys can undergo various types of structural changes at micro- and nanometer length scales [1]. At high doses (>10 dpa, displacements per atom) and at temperatures between 300 °C and 700 °C, one of these changes is void formation, which can lead to macroscopic swelling of tens of percent [2–4]. More than a few percent of swelling is typically incompatible with the demands of structural components in nuclear systems [5]. One avenue to develop swelling-resistant materials relies on the introduction of a high density of sinks for mobile point defects [5,6]. Increased sink strengths have been achieved in materials with high surface-to-volume ratios of interface sinks such as multilayered Cu-Nb composites [7–9].

Austenitic stainless steels (SS) are attractive for nuclear reactor applications [5,10] but can be prone to void swelling [11]. Tangled dislocations introduced by cold-work [12] can act as sinks and have been shown to reduce swelling in SS [13–15,4]. However, after a threshold dose of about 30 dpa for cold-worked SS to about 50 dpa for cold-worked Ti-modified SS, swelling rates increase and become more similar to the ones of annealed SS [16]. Grain boundaries, in particular random high-angle grain boundaries, can also be effective sinks for radiation defects [17] and extend the low swelling regime to higher radiation doses. Several recent studies using ion irradiation have shown that ultra-fine grained alloys have significant swelling resistance up to 80 dpa as compared to their coarse grained counterparts [18,19]. However, ultra-fine grained alloys tend to have very low ductility [20], which is undesirable for nuclear reactor applications. Thus, alternative types of internal interfaces such as deformation twin boundaries may be explored for enhancing swelling resistance without compromising ductility.

In austenitic steels, twins may be introduced during annealing, thin film growth, or deformation. Thermo-mechanical treatments can be used to promote the formation of annealing twins in SS [21]. The density of twin boundaries (area of twin boundaries per unit volume) is however low due to the width of annealing twins. A high density of twin boundaries can be achieved with in laboratory-scale thin films produced by processes such as electrodeposition or physical vapor deposition (growth twins) [22], but these processes are not suitable for fabricating components. High densities of twin boundaries can however be achieved in components via deformation twinning (see reviews [23] and [24]). By relying on large strain rate deformation followed by annealing at moderate temperatures (e.g., 700 °C), several studies have demonstrated that high densities of twin boundaries can be achieved while maintaining high ductility levels in SS [25–28].

Deformation twin boundaries are generally Σ3 {111} coherent twin boundaries (CTBs) and occasionally Σ3 {112} symmetric incoherent twin boundaries (ITBs) at locations where the twin has ledges or tips [29]. CTBs are considered as very weak sinks. For example, irradiation experiments showed insignificant or no void-denuded zone in the vicinity of CTBs [30–33] and low or insignificant radiation-induced segregation (RIS) across CTBs as compared to random high-angle grain boundaries [31,34–39]. The weak sink strength is in particular related to the fact that CTBs have a very low free energy among Σ3 ⟨110⟩ tilt boundaries [40]. First-principle simulations of point defect formation

* Corresponding author.
E-mail address: mericdebelle@wisc.edu (G. Meric de Bellefon).

https://doi.org/10.1016/j.scriptamat.2018.09.030

energies and recombination ranges at CTBs in Cu support the experimental observations of their low sink strength [32,41]. However, observations of the radiation response of CTBs reported in the literature are typically conducted on isolated CTBs from wide annealing twins. It can then be hypothesized that the sink effect of an isolated CTB is too weak to be detectable, but that a high density of CTBs could combine to produce a significant sink strength and impact the radiation response. Low-dose ion irradiation experiments of nanotwinned Ag [42–45] and nanotwinned Cu [46] thin films produced by physical vapor deposition [47] support this hypothesis. In this paper, the effectiveness of deformation twin boundaries as sinks for point defects is reported in an ion-irradiated SS. It will be shown that regions containing closely-spaced twin boundaries exhibit a higher resistance to void swelling than regions with no twins.

The test material for this study was austenitic 316 SS of the following composition (wt%): 14-Ni, 18-Cr, 3.0-Mo, 0.10-Si, 0.94-Mn, 0.04-C, 0.009-N. A bar of the test material was annealed at 1050 °C for 30 min, water quenched, and cold-rolled with a 30% thickness reduction at room temperature to introduce deformation twins. A bulk sample for irradiation was prepared by cutting a section perpendicular to the rolling direction, polishing it down progressively to 1200 grit surface finish, and electro-polishing it with a standard A2 electrolyte at −15 °C for 10 min to remove about 200 μm of materials from the surface, thereby removing all defects induced by mechanical polishing. A control sample was prepared from a non-cold-rolled bar. The electro-polished surface of the bulk sample was irradiated with 3.5-MeV Fe^{2+} ions at 500 °C to a fluence of about 5×10^{16} ions·cm^{-2} (about 50 dpa at peak damage depth of 1 μm as estimated with SRIM [48]) at a flux of about 5×10^{12} ions·cm^{-2}·s^{-1}. The ion beam was not rastered to better emulate neutron irradiation [49]. Cross-sectional specimens for transmission electron microscopy (TEM) were extracted from the bulk samples and prepared by focused ion beam (FIB) machining using 30 kV Ga^+ ions followed by 5 kV Ga^+ ions. The FIB instrument was a Zeiss Auriga FIB equipped with a Ga liquid metal ion source and a Schottky field emission scanning electron microscope (SEM). Conventional TEM observations of voids were performed using an FEI Tecnai TF-30 equipped with a Schottky field-emission electron gun operating at 300 kV. Chemical segregation at boundaries was measured using an energy-dispersive X-ray spectroscopy (EDS) detector attached to an FEI Titan aberration-correct Scanning TEM equipped with a Schottky field-emission electron gun operating at 200 kV. Electron Back Scatter Diffraction (EBSD) mapping was performed on a FEI Helios G4 UX Extreme High-Resolution Field Emission Scanning Electron Microscope equipped with an EDAX Hiraki Super EBSD camera and the TEAM EBSD data collection software. An accelerating voltage of 30 kV, a current of 26 nA, and a step size of 15 nm were used. The working distance was about 4 mm. Scans were performed using 5 × 5 binning at a rate of ~200 points per second.

The location of the cross-sectional specimen on the surface of the bulk sample from the cold-rolled test material is shown in Fig. 1a and its transmission EBSD map is shown in Fig. 1b. As seen in the micrograph, the specimen has two main grains: one heavily twinned grain on the left and an un-twinned grain on the right. The void distribution was analyzed using the through focus imaging condition [50]. Under this condition, the under-focused images have a dark Fresnel fringe around the voids, the over-focused images have a bright Fresnel fringe around the voids, and the in-focus images show voids with negligible contrast. Better void contrast is usually obtained in kinematical imaging conditions [50]. Under this imaging condition, the background contrast for dislocations and twin boundaries is weak. An example over-focused, kinematical image is shown in Fig. 2a. The same region in in-focus, dynamical imaging condition to reveal twin boundaries at a higher contrast is shown in the rectangle embedded in Fig. 2b.

The main observation from the micrographs is that the void density is strongly affected by the presence of deformation twin boundaries. Some regions with a high density of twin boundaries exhibit full void

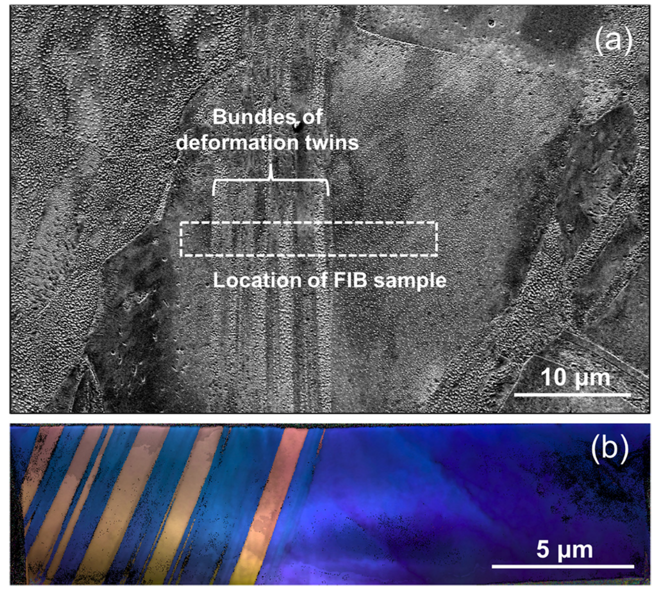

Fig. 1. (a) SEM micrograph of the surface of a 30% cold-rolled 316 austenitic stainless steel subject to 3.5 MeV Fe^{2+} irradiation at 500 °C to a total fluence of 6×10^{16} cm^{-2}. The location of the cross-sectional specimen used in this study is indicated by the white rectangle. (b) Transmission EBSD map of the cross-sectional specimen shows some large deformation twins on the left grain. The color indicates the crystal orientation with respect to a random direction. (For interpretation of the references to color in this figure legend, the reader is referred to the web version of this article.)

suppression as shown in the center-left and far right regions of Fig. 2a. Some regions with a moderate density of twin boundaries show less pronounced void suppression, which is typically associated with a somewhat degraded deformation twin microstructure likely caused by radiation-induced de-twinning [51]. To quantify the role of deformation twin boundaries on swelling, void swelling was estimated and compared to the local density of twin boundaries. Void swelling was estimated by approximating voids as spheres and measuring the diameters of all voids in regions of interests. Because irradiation was performed on bulk samples, the pre-irradiation twin boundary density cannot be known. However, numerous observations of deformation twins in un-irradiated areas reveal that they almost always run from grain boundary to grain boundary. The density of twin boundaries just below the damage zone (at the top of the un-irradiated zone) was therefore used to estimate the pre-irradiation twin boundary density. In regions with closely-spaced twins, this pre-irradiation twin boundary density is uniform with a mean spacing between twin boundaries of approximately 20 nm. These regions are clearly separated from one another by wide regions with no twin boundary. Void sizes were measured separately for two types of regions: regions with closely-spaced twin boundaries and regions with no twin boundary, as defined by the top of the un-irradiated zone. Using this convention, Fig. 2c shows estimated swelling amounts in these regions. On average, the swelling is reduced by a factor of three in the regions with closely-spaced twin boundaries (0.09% swelling vs. 0.28% swelling). By comparison, swelling in the control, non-cold-rolled material was about 3%. The specimen thickness was measured to be about 150 nm using the Electron Energy-Loss Spectrometry method [52]. The measured thicknesses were similar in regions with and without voids. EDS measurements of chemical concentration across isolated and closely-spaced CTBs showed moderate RIS - about 5 wt%-Cr depletion, as compared to 15 wt%-Cr depletion at a random high angle grain boundary, as shown in Fig. 3.

The driving force for void formation is a supersaturation of vacancies [1]. This supersaturation of vacancies is caused by the formation of vacancies through displacement cascades and the preferential absorption of self-interstitial atoms by dislocations [53]. The evolution of swelling with dose usually occurs in two regimes: a low-swelling transient